EXTENDING ISOBAR MODEL FOR KAON PHOTOPRODUCTION UP TO 16 GeV

T. Mart and T. Wijaya

Jurusan Fisika, FMIPA, Universitas Indonesia, Depok 16424, Indonesia

(Received December 13, 2002; revised version received February 18, 2003)

We extend the isobar model for kaon photoproduction to consider higher energy data by combining the model with a Regge approach. The extended model works nicely between threshold and 16 GeV. It is shown that model with crossing symmetric Born terms leads to a better description of experimental data. We use the model to calculate contributions of kaon channels to the Gerasimov–Drell–Hearn sum rule up to 16 GeV.

PACS numbers: 13.60.Le, 11.55.Hx, 13.40.Em, 14.20.Dh

1. Introduction

The isobar model has been proven very powerful for studying photo- and electroproduction of mesons. Using an isobar model one has the opportunity to study some phenomenological aspects related to the process, *i.e.*, the electromagnetic and hadronic form factors, the excited baryon and meson resonances, as well as individual contributions to the anomalous magnetic moment of the nucleon in the Gerasimov–Drell–Hearn (GDH) sum rule. Reference [1], *e.g.*, has identified a missing nucleon resonance D_{13} with mass (width) of 1895 (372) MeV by analyzing the new $\gamma + p \to K^+ + \Lambda$ data in the framework of isobar model.

Despite of their success, isobar models usually work only up to photon lab energy $E_\gamma^{\rm lab} = 2$ GeV. Beyond this energy region most models become deficient and show divergence, unless some hadronic form factors are considered in the hadronic vertices, and their roles are traditionally substituted by Regge approaches. However, a brief inspection to the particle data book reveals that almost 50% of baryon resonances are observed with masses between 2 and 3 GeV, which is clearly beyond the regime of isobar models. Since Regge model cannot be used to investigate these resonances, a new resonance driven mechanism explaining the electromagnetic production of meson in this energy region should be established.

Moreover, an extension of isobar model to higher energies becomes an urgent task if, for instance, we consider the calculation of the GDH sum rule. Basically, the sum rule involves an integral from reaction thresholds up to $E_\gamma^{\rm lab} = \infty$. However, due to the limitation of the model, usually one has to stop at or below $E_\gamma^{\rm lab} = 2$ GeV, which means disregarding the higher energy contributions. As an example, Ref. [2] has calculated contributions of kaon–hyperon final states to the GDH sum-rule up to 2 GeV. Thus, the accuracies of such calculation would strongly depend on the upper limitation of the model.

At Jefferson Lab, kaon electroproduction experiment has been performed with total c.m. energy $W = 3$ GeV [3]. A proposal for upgrading the accelerator to reach 12 GeV has been also discussed [4]. To this end, no isobar model has been proposed to investigate physics of the process at this energy.

For this purpose we will follow the method used in Ref. [5], *i.e.* combining the conventional isobar model with a Regge approach. We note that this procedure has been successfully applied to a multipole analysis of single-pion photoproduction between threshold and $E_\gamma^{\rm lab} = 16$ GeV.

2. Formalism

With the convention of four-momenta

$$\gamma(p_\gamma) + N(p_N) \longrightarrow K(p_K) + Y(p_Y)\,, \tag{1}$$

the transition matrix for both isobar and Regge models for kaon photoproduction can be written in the form of

$$M_{fi} \;=\; \bar{u}(\boldsymbol{p}_Y, s_Y) \sum_{i=1}^{4} A_i \; M_i \; u(\boldsymbol{p}_N, s_N)\,, \tag{2}$$

where the gauge and Lorentz invariant matrices M_i are given by [6]

$$M_1 \;=\; \gamma_5 \not{\epsilon} \not{p}_\gamma, \tag{3}$$
$$M_2 \;=\; 2\gamma_5 (p_K \cdot \epsilon \; p_N \cdot p_\gamma - p_K \cdot p_\gamma \; p_N \cdot \epsilon)\,, \tag{4}$$
$$M_3 \;=\; \gamma_5 (p_K \cdot p_\gamma \not{\epsilon} - p_K \cdot \epsilon \not{p}_\gamma)\,, \tag{5}$$
$$M_4 \;=\; i\varepsilon_{\mu\nu\rho\sigma} \gamma^\mu p_K^\nu \epsilon^\rho p_\gamma^\sigma\,, \tag{6}$$

and ϵ indicates the photon polarization. The amplitudes A_i are obtained from Feynman diagrams by using the vertex factors and propagators given in Ref. [7,8].

The Born amplitudes for kaon photoproduction are given by

$$\begin{aligned} A_1^{\rm Born} &= -\frac{eg_{KYN}}{s-m_N^2}\left(Q_N+\kappa_N\frac{m_N-m_Y}{2m_N}\right)F(\Lambda,s) \\ &\quad -\frac{eg_{KYN}}{u-m_Y^2}\left(Q_Y+\kappa_Y\frac{m_Y-m_N}{2m_Y}\right)F(\Lambda,u) \\ &\quad -(1-|Q_Y|)\frac{eG_{KY'N}}{u-m_{Y'}^2}\,\frac{m_{Y'}-m_N}{m_{Y'}+m_Y}\,F(\Lambda,u)\,, \qquad (7) \\ A_2^{\rm Born} &= \frac{2eg_{KYN}}{t-m_K^2}\left(\frac{Q_N}{s-m_N^2}+\frac{Q_Y}{u-m_Y^2}\right)\widetilde{F}\,, \qquad (8) \\ A_3^{\rm Born} &= \frac{eg_{KYN}}{s-m_N^2}\,\frac{\kappa_N F(\Lambda,s)}{2m_N}-\frac{eg_{KYN}}{u-m_Y^2}\,\frac{\kappa_Y F(\Lambda,u)}{2m_Y} \\ &\quad -(1-|Q_Y|)\frac{eG_{KY'N}}{u-m_{Y'}^2}\,\frac{F(\Lambda,u)}{m_{Y'}+m_Y}\,, \qquad (9) \\ A_4^{\rm Born} &= \frac{eg_{KYN}}{s-m_N^2}\,\frac{\kappa_N F(\Lambda,s)}{2m_N}+\frac{eg_{KYN}}{u-m_Y^2}\,\frac{\kappa_Y F(\Lambda,u)}{2m_Y} \\ &\quad +(1-|Q_Y|)\frac{eG_{KY'N}}{u-m_{Y'}^2}\,\frac{F(\Lambda,u)}{m_{Y'}+m_Y}\,, \qquad (10) \end{aligned}$$

where Q_N and Q_Y denote the charges of the nucleon and the hyperon in $+e$ unit, while κ_N, κ_Y, and κ_T indicate the anomalous magnetic moments of the nucleon, hyperon, and the transition of $\Sigma^0\Lambda$. It is understood that $Y' = \Sigma^0$ $[\Lambda]$ for $K\Lambda$ $[K\Sigma^0]$ production. The form factors $F(\Lambda,x)$, with $x = s,t,u$, and $\widetilde{F}$ indicate inclusion of hadronic structures in the corresponding vertices. It is a well-known fact that inclusion of this structure in the model leads to a violation of gauge invariance. However, in order to take into account the fact that baryons and mesons are not point-like, including hadronic form factors in the model is inevitable. There have been several methods to alleviate this problem, two of them have been proposed by Ohta [9] and Haberzettl [10]. To restore gauge invariance Ohta has derived an additional current corresponding to a contact term by making use of minimal substitution. However this method was found by Haberzettl to be too restrictive, since it amounts to removing any vertex dressing from the dominant electric contributions which clearly removes the desirable effects of suppressing the divergence of the amplitude. In our notation Ohta's method corresponds to $\widetilde{F} = 1$, thus provides no cut-off for higher energies. In the Haberzettl's prescription $\widetilde{F}$ can have arbitrary form, nevertheless a more "democratic" choice was chosen as [11]

$$\widetilde{F} \;=\; a_1F_1(s)+a_2F_2(u)+a_3F_3(t) \quad \text{with} \quad a_1+a_2+a_3 \;=\; 1\,. \qquad (11)$$

It has been shown [11] that this choice is more flexible and superior to Ohta's approach. Indeed, most of the modern studies of kaon photoproduction used Haberzettl's method in an effective Lagrangian framework [11–13].

The $K^*(892)$ and $K_1(1270)$ vector meson poles are also included in the t-channel, since previous studies found that their roles are significant in the $K^+\Lambda$ photoproduction [7,8]. The low-energy resonance part of the $K\Lambda$ operator includes three states that have been found to have significant decay widths into the $K^+\Lambda$ channel, the $S_{11}(1650)$, $P_{11}(1710)$, and $P_{13}(1720)$ resonances. Due to their isospin structure the $K\Sigma$ photoproduction channels can involve the excitation of N^* as well as Δ states. In this model we include two spin $1/2$ Δ, the $S_{31}(1900)$ and $P_{31}(1910)$ states. In Ref. [14] it is shown that the agreement with data is significantly improved by including a $P_{13}(1720)$ intermediate state in $K\Sigma$ channels. An excellent agreement between low energy experimental data and model prediction has been achieved, where it is then found that a new, missing, $D_{13}(1895)$ nucleon resonance appears naturally in order to explain the apparent structure in the total cross section of the SAPHIR data in the $K^+\Lambda$ channel [1]. These resonance terms are all gauge-invariant independently and, therefore, do not depend on different prescriptions of restoring gauge invariance. Their amplitudes can be found in the previous works [7,8]. In general we have

$$A_i^{\rm iso} \;=\; A_i^{\rm Born} + A_i^{\rm res}\,, \qquad i = 1,\ldots,4\,, \tag{12}$$

where $A_i^{\rm res}$ denotes contributions from resonance terms including the t-channel poles.

Very recently, Davidson and Workman [15] noticed that the gauge method of Haberzettl [11] could create a pole in the background part and the corresponding Born terms are not crossing symmetric. We have fixed this problem in our model by taking a special form for the $\widetilde{F}$ form factor, *i.e.*

$$\begin{aligned}\widetilde{F} \;=\; & F_1(s) + F_1(u) + F_3(t) + F_1(s)F_1(u)F_3(t) \\ & -F_1(s)F_1(u) - F_1(s)F_3(t) - F_1(u)F_3(t)\,,\end{aligned} \tag{13}$$

as suggested by Ref. [15], and refitted the low energy data to obtain the coupling constants. The result has been partly reported in Ref. [16]. Thus, in conclusion, in the low energy region we use an isobar model that includes hadronic form factors, satisfies gauge invariance and crossing symmetry, and is free of poles.

For the higher energy region, we use the Regge model developed by the Saclay group to explain high energy pion and kaon photoproduction ($E_\gamma^{\rm lab}$ between 4 and 16 GeV) [17]. The model exploits the K and K^* trajectories and includes the electric term of the s- and u-channel diagrams

to ensure gauge invariance of the amplitude. In our notation the amplitudes for this model read

$$A_1^{\rm Reg} = -\frac{eg_{KYN}\,Q_N}{s-m_N^2}\,(t-m_K^2)\,\mathcal{P}_{\rm Reg}^{K} - \frac{C_{K^*}G_T t}{M(m_N+m_Y)}\,\mathcal{P}_{\rm Reg}^{K^*}\ , \quad (14)$$

$$A_2^{\rm Reg} = \frac{2eg_{KYN}\,Q_N}{s-m_N^2}\,\mathcal{P}_{\rm Reg}^{K} + \frac{C_{K^*}G_T}{M(m_N+m_Y)}\,\mathcal{P}_{\rm Reg}^{K^*}\ , \quad (15)$$

$$A_3^{\rm Reg} = -\frac{C_{K^*}G_T(m_N-m_Y)}{M(m_N+m_Y)}\,\mathcal{P}_{\rm Reg}^{K^*}\ , \quad (16)$$

$$A_4^{\rm Reg} = \frac{C_{K^*}G_V}{M}\,\mathcal{P}_{\rm Reg}^{K^*}\ , \quad (17)$$

where

$$\mathcal{P}_{\rm Reg}^{K} = \left(\frac{s}{s_0}\right)^{\alpha_K(t)} \frac{{\rm e}^{-i\pi\alpha_K(t)}}{\sin(\pi\alpha_K(t))}\frac{\pi\alpha'_K}{\Gamma(1+\alpha_K(t))}\,, \quad (18)$$

and

$$\mathcal{P}_{\rm Reg}^{K^*} = \left(\frac{s}{s_0}\right)^{\alpha_{K^*}(t)-1} \frac{{\rm e}^{-i\pi\alpha_{K^*}(t)}}{\sin(\pi\alpha_{K^*}(t))}\frac{\pi\alpha'_{K^*}}{\Gamma(\alpha_{K^*}(t))}\,, \quad (19)$$

with α^K and α^{K^*} the K and K^* trajectories given in Ref. [17] and C_{K^*} the isospin coefficient for the K^* exchange [19]. In Eqs. (14)–(17) $M = 1$ GeV is inserted to make the coupling constants G_V and G_T dimensionless. By taking the standard trajectory equations for K and K^* and fitting their coupling constants a good agreement with high energy data is achieved [17].

Following Ref. [5], for the transition region, we modify the amplitudes A_i in Eq. (12) by combining the two models

$$A_i^{\rm trans} = \frac{1}{s_1-s_2}\left\{(s-s_2)\;A_i^{\rm iso} + (s_1-s)\;A_i^{\rm Reg}\right\}, \qquad i=1,\ldots,4\,, \quad (20)$$

where $s = (p_\gamma + p_N)^2 = W^2$. For this study we limit the transition region within W = 2–3 GeV, and therefore $s_1 = 4$ GeV^2 and $s_2 = 9$ GeV^2, a region where we expect that the future experimental data will provide new information on whether or not higher lying resonances have significant decay widths to $K\Lambda$ and $K\Sigma$ channels.

We note that another alternative to extend the model to the higher energy region is by reggeizing the t-channels of the operator [18], *i.e.* multiplying the t-channels with $P_{\rm Reg}\,(t-m_{K^*}^2)$, where $P_{\rm Reg}$ indicates the Regge propagator given by Eq. (19). It is shown [18] that this procedure can eliminate the divergence provided that the background part of the model

does not violently increase as a function of energy, since at higher energies the t-channel resonances dominate all contributions [6] and, therefore, are responsible for the divergent behavior. Details of this procedure and the corresponding result will be published in the future.

3. Results and discussions

The result for all three proton channels is shown in Fig. 1. Clearly, in all channels, the low energy isobar model starts to diverge at W slightly above 2 GeV and the discrepancy with the data at region III is not surprising. The Regge model fits higher energy data, but overpredicts the low energy ones in $K^+\Lambda$ and $K^0\Sigma^+$ channels, whereas it underestimates the $K^+\Sigma^0$ data. The different behavior shown by the Regge model in $K^+\Sigma^0$ and $K^0\Sigma^+$ channels

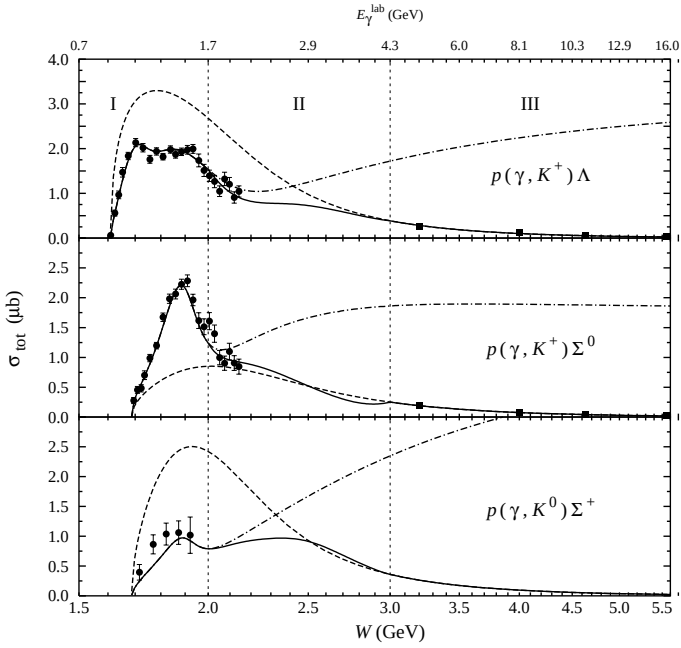

Fig. 1. Total cross section for kaon photoproduction on the proton. The dash-dotted line shows the isobar model which has been fitted to experimental data up to $E_\gamma^{\rm lab} = 2.2$ GeV [16], dashed lines display the Regge model fitted to $E_\gamma^{\rm lab} =$ 4–16 GeV [17], while solid lines are the extended model, valid from threshold up to $E_\gamma^{\rm lab} = 16$ GeV. The new SAPHIR data [20] are denoted by solid circles, old data [21] are shown by solid squares. Regions I, II, and III correspond to the isobar, transition, and Regge domains, respectively. Note the logarithmic scale for the W-axis.

can be understood from the coupling constants relation in the two channels [19]. Combining the two approaches by using Eq. (20) clearly produces the expected result, where we see a continuous transition from region I to region II and III. Unfortunately, Eq. (20) does not guarantee a smooth inter-region transition in the total cross section, as shown, *e.g.*, in the $K^+\Sigma^0$ channel of Fig. 1. This problem, however, could be alleviated if we had experimental data in the transition region, with which refitting the coupling constants would improve the extended model. For the present we cannot see any indication of resonance in this region, since no intermediate state is included at this kinematics. Future experimental data with accuracies comparable to SAPHIR data would be sufficient to shed important information at this region.

In Fig. 2 we compare the extended model with different gauge methods of Haberzettl and Davidson–Workman (DW), along with the result obtained from refitting coupling constants in DW method to all data, where in the lat-

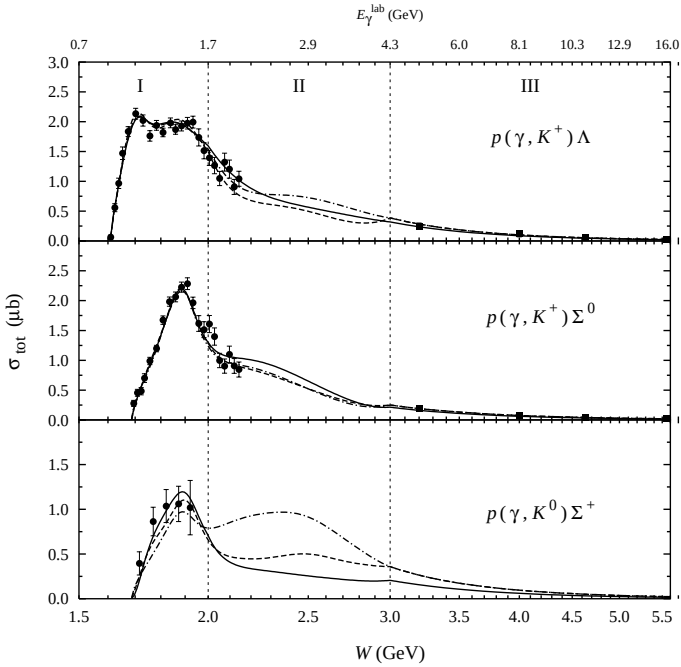

Fig. 2. Total cross section for kaon photoproduction on the proton. Dashed lines show the extended model with the Haberzettl's gauge invariant prescription [11], dash-dotted lines are obtained by using the Davidson–Workman (DW) gauge-invariant method [15], while solid lines display the extended model with DW recipe refitted to all available data from threshold up to $E_\gamma^{\rm lab} = 16$ GeV. Everything else is as in Fig. 1.

ter we could investigate the dependency and behavior of coupling constants in the isobar and Regge models, and expect a substantial improvement in the whole energy region. Interestingly, Fig. 2 indicates that measurement of the $K^0\Sigma^+$ channel with total c.m. energy between 2 and 3 GeV is well suited for testing the two gauge prescriptions.

With exception of the $K^0\Sigma^+$ channel the improvement by refitting to all data shown in Fig. 2 seems to be insignificant. However, differential cross sections shown in Figs. 3, 4, 5 reveal more information. In general, higher energy differential cross sections show a forward peaking behavior. The Haberzettl prescription results in a significant discrepancy with experimental data, especially at $W = 2.817$ GeV in the $K^+\Lambda$ channel. Although the

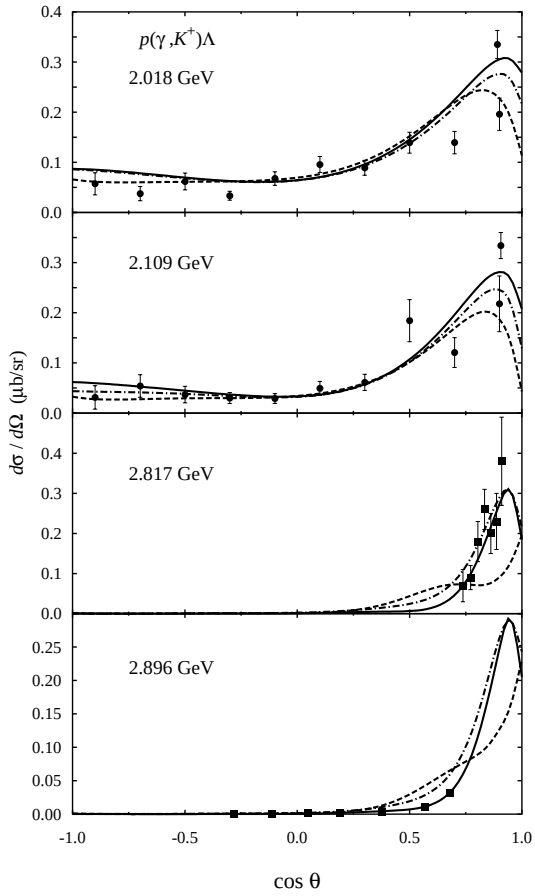

Fig. 3. Differential cross section for the $p(\gamma, K^+)\Lambda$ channel. Notation is the same as in Fig. 2. Experimental data for $W = 2.018$ and 2.109 GeV are from Ref. [20], while those for $W = 2.817$ and 2.896 GeV come from Refs. [22] and [23], respectively.

result indicates that the crossing symmetry in the Born terms could become an important constraint to the model, this is still unclear in the case of $K^+\Sigma^0$ due to the lack of data in the forward region. At this kinematics all calculations obviously deviate from $K^+\Sigma^0$ data, indicating that a further analysis might be required as soon as experimental data become available.

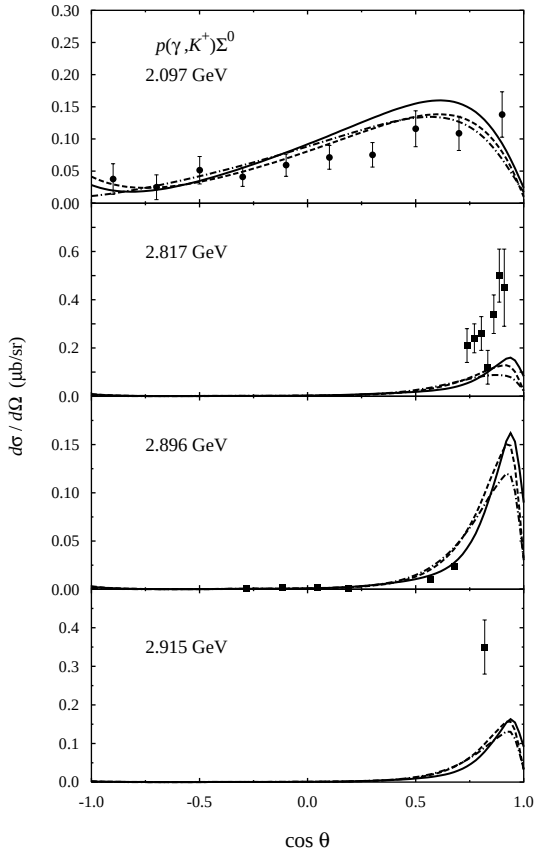

Fig. 4. Differential cross section for the $p(\gamma, K^+)\Sigma^0$ channel. Notation is the same as in Fig. 3. The datum at $W = 2.915$ GeV is from Ref. [22].

Figure 5 shows that in the transition region, kaon angle between 0 and 60 degrees would be the best kinematics to examine the validity of our predictions. Thus, from the three figures we may conclude that measurement of differential cross sections at the transition region is advocated, especially at forward angles.

Figure 6 shows polarization of the recoiled hyperon in the proton channels, where we can see sizable differences between models in the Λ, Σ^0 and Σ^+ polarizations. In the Λ case, it is obvious that the symmetric Born terms

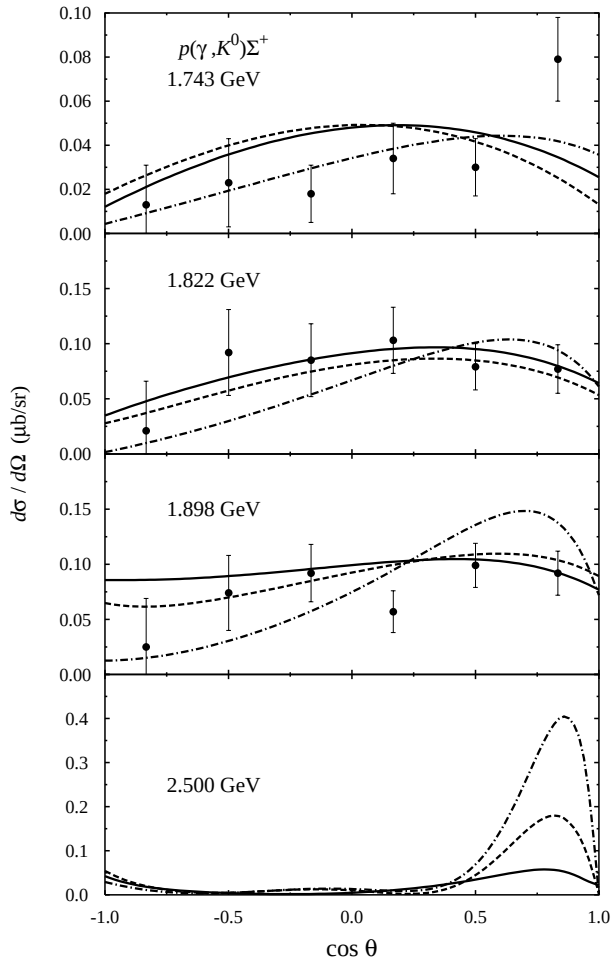

Fig. 5. Differential cross section for the $p(\gamma, K^0)\Sigma^+$ channel. Notation is the same as in Fig. 3. Data are from Ref. [20].

lead to a slightly better description of data in the low energy region, while in the opposite case we cannot see the difference since we use the same Regge model. The effect of refitting all coupling constants (including those of the Regge model) is nevertheless substantial at this energy. Unfortunately, the available data are not sufficiently precise to single out these models. The predicted Σ^+ polarizations show almost similar angular distribution and the accuracies of experimental data do not also differentiate the models.

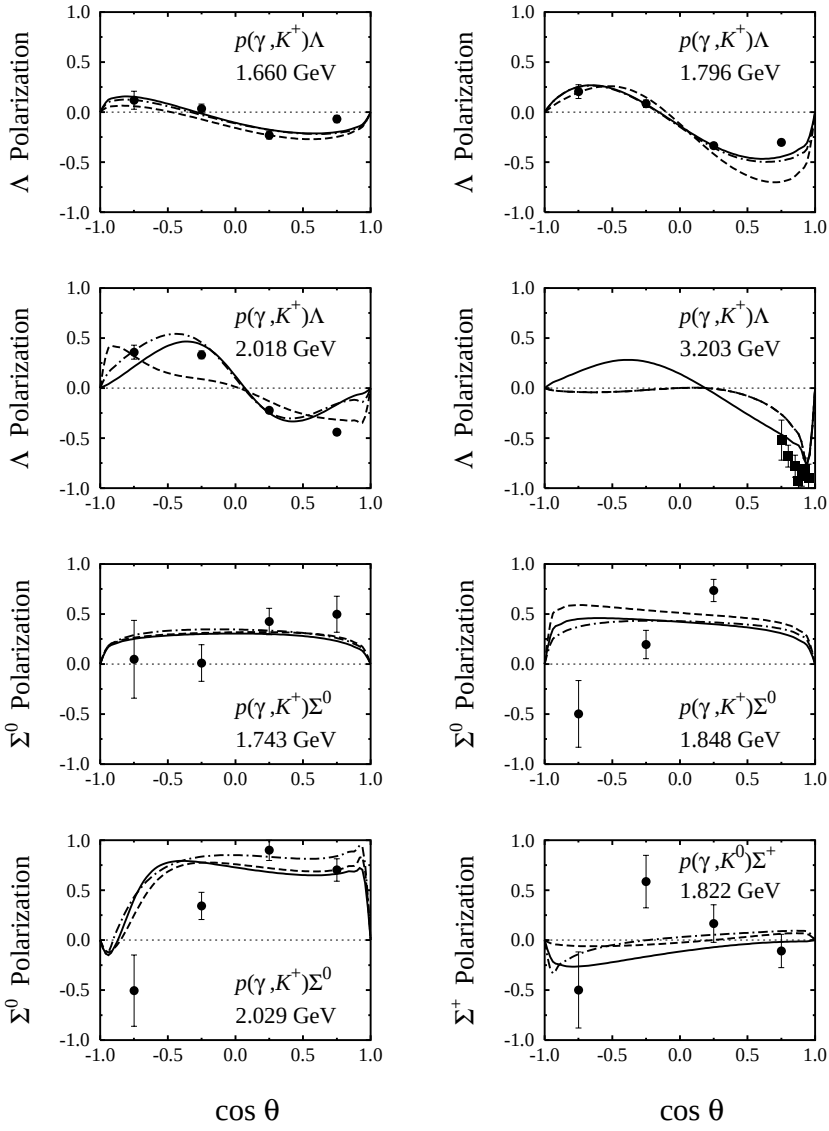

Fig. 6. Polarization of the recoiled hyperon in proton channels. Notation is as in Fig. 3. Except for $W = 3.203$ GeV [24], data come from SAPHIR experiments [20].

4. Contributions to the Gerasimov–Drell–Hearn sum rule

Using the extended model we can calculate contributions of kaon channels to the Gerasimov–Drell–Hearn (GDH) sum rule on the proton for $E_\gamma^{\rm lab}$ from threshold up to 16 GeV. The GDH sum rule (for a review see Ref. [25])

relates the anomalous magnetic moment of the nucleon κ_N to the difference of its polarized total photoabsorption cross section

$$-\frac{2\pi^2\alpha}{m_N^2}\,\kappa_N^2 \;=\; \int\limits_0^\infty \frac{d\nu}{\nu}\,\left[\,\sigma_{1/2}(\nu)-\sigma_{3/2}(\nu)\,\right]\,, \tag{21}$$

where $\sigma_{1/2}$ and $\sigma_{3/2}$ represent the cross sections for the possible spin combinations of the proton and photon (*i.e.*, $\sigma_{1/2}$ for total spin $=\frac{1}{2}$ and $\sigma_{3/2}$ for total spin $=\frac{3}{2}$), α is the fine structure constant, $\nu = E_\gamma^{\rm lab}$, and m_N the mass of the nucleon.

In photoproduction processes, however, the spin-dependent cross sections are related to the unpolarized total cross section by

$$\sigma_{\rm T}(\nu) \;=\; \frac{\sigma_{3/2}(\nu)+\sigma_{1/2}(\nu)}{2} \tag{22}$$

and to the transverse–transverse response function [26] by

$$\sigma_{\rm TT'}(\nu) \;=\; \frac{\sigma_{3/2}(\nu)-\sigma_{1/2}(\nu)}{2}\,, \tag{23}$$

which can be measured by using polarized real photons and polarized target. In terms of polarization observables the latter corresponds to the double polarization E [27]. By combining Eq. (21) and Eq. (23) we obtain

$$\kappa_N^2 \;=\; \frac{m_N^2}{\pi^2\alpha}\int\limits_0^\infty \frac{d\nu}{\nu}\,\sigma_{\rm TT'}(\nu)\,. \tag{24}$$

The response functions $\sigma_{\rm TT'}$ for all three proton channels are shown in Fig. 7, along with the unpolarized total cross sections $\sigma_{\rm T}$ for comparison. Although the total contribution is relatively small compared to other channels, such as π and η channels, Fig. 7 obviously illustrates that contributions from the transition region (II) cannot be neglected from the calculation, while contributions from the Regge domain are relatively small. This is more elucidated in Table I, where we can see that more than 20% of the total contribution come from the transition region, while the Regge domain contributes just less than 4%. The value obtained in this calculation (2.533 μb) is in fact smaller than that of previous study using an isobar model without crossing symmetric constraint. Nevertheless, this can be immediately understood from the predicted $\sigma_{\rm TT'}$ shown in Fig. 7, which cover smaller area compared to the previous calculation [2], especially in the case of $K^0\Sigma^+$ channel, where the oscillating difference of the cross sections reduces the GDH integral significantly. Experimental data of $\sigma_{\rm TT'}$ from threshold up to $W = 3$ GeV with error-bars less than 10% would be demanded to settle this problem.

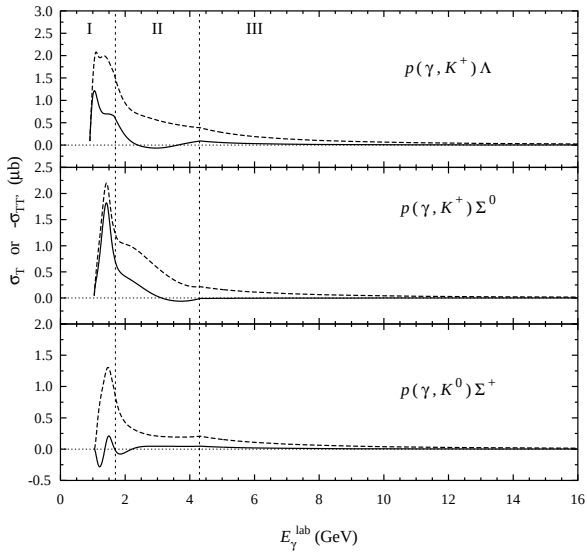

Fig. 7. Total cross sections σ_T (dashed lines) and response functions $-\sigma_{TT'}$ (solid lines) for kaon photoproduction on the proton. All curves are obtained from the model corresponding to the solid line in Fig. 2. Experimental data for σ_T are not shown for convenience.

TABLE I

Contributions of kaon photoproduction on the proton to the GDH integral [Eq. (21)] in μb. For comparison, the l.h.s. of Eq. (21) is equal to -204 μb.

Region	$K^+\Lambda$	$K^+\Sigma^0$	$K^0\Sigma^+$	Total
I	0.989	0.958	-0.039	1.908
II	0.169	0.347	0.028	0.544
III	0.056	-0.008	0.033	0.081
All	1.214	1.297	0.022	**2.533**

5. Conclusion

In conclusion, we have successfully extended an isobar model to consider higher energy kaon photoproduction data up to 16 GeV by combining the model with a Regge approach in the transition region $W = 2-3$ GeV. Using this extended model we have refined the calculation of the kaon-hyperon final states contributions to the GDH sum-rule on the proton and we found that contributions from the transition region are still significant, *i.e.* up to 20% of those from the low energy region. Accurate measurements of total and differential cross sections between threshold and 3 GeV as well as experiments with polarized photon and target are urgently required to eliminate some uncertainties in this calculation.

The authors thank Dr. Olaf Hanstein for useful discussion on the transition from isobar to Regge model. This work was supported in part by the QUE (Quality for Undergraduate Education) project.

REFERENCES

[1] T. Mart, C. Bennhold, *Phys. Rev.* **C61**, 012201(R) (2000).
[2] S. Sumowidagdo, T. Mart, *Phys. Rev.* **C60**, 028201 (1999).
[3] Exclusive Kaon Electroproduction in Hall B at 6 GeV, JLab Experiment E-00-112, D. Carman (spokesperson).
[4] *Proceedings of the Workshop on Jefferson Lab Physics and Instrumentation with 6–12 GeV Beams*, eds S. Dytman, H. Fenker, P. Roos, Jefferson Lab, Newport News, VA, June 1998.
[5] I.M. Barbour, R.L. Crawford, N.H. Parsons, *Nucl. Phys.* **B141**, 253 (1978).
[6] F.X. Lee, T. Mart, C. Bennhold, H. Haberzettl, L.E. Wright, *Nucl. Phys.* **A695**, 237 (2001).
[7] R.A. Adelseck, B. Saghai, *Phys. Rev.* **C42**, 108 (1990).
[8] R.A. Adelseck, C. Bennhold, L.E. Wright, *Phys. Rev.* **C32**, 1681 (1985).
[9] K. Ohta, *Phys. Rev.* **C40**, 1335 (1989).
[10] H. Haberzettl, *Phys. Rev.* **C56**, 2041 (1997).
[11] H. Haberzettl, C. Bennhold, T. Mart, T. Feuster, *Phys. Rev.* **C58**, 40 (1998).
[12] T. Feuster, U. Mosel, *Phys. Rev.* **C59**, 460 (1999).
[13] B.S. Han, M.K. Cheoun, K.S. Kim, I.T. Cheon, *Nucl. Phys.* **A691**, 713 (2001).
[14] T. Mart, *Phys. Rev.* **C62**, 038201 (2000).
[15] R.M. Davidson, R. Workman, *Phys. Rev.* **C63**, 025210 (2001).
[16] T. Mart, C. Bennhold, H. Haberzettl, in Proceedings of the International Symposium on Meson–Nucleon Physics and the Structure of the Nucleon, GWU, Washington D.C., July 2001; *π-N Newslett.* **16**, 86 (2002).
[17] M. Guidal, J.M. Laget, M. Vanderhaeghen, *Nucl. Phys.* **A627**, 645 (1997).
[18] T. Mart, S. Sumowidagdo, C. Bennhold, H. Haberzettl, `nucl-th/0002036`.
[19] T. Mart, C. Bennhold, C.E. Hyde-Wright, *Phys. Rev.* **C51**, 1074 (1995).
[20] SAPHIR Collaboration, M.Q. Tran *et al.*, *Phys. Lett.* **B445**, 20 (1998); S. Goers *et al.*, *Phys. Lett.* **464**, 331 (1999).
[21] A. M. Boyarski *et. al.*, *Phys. Rev. Lett.* **22**, 1131 (1969).
[22] V.B. Elings *et al.*, *Phys. Rev.* **156**, 1433 (1967).
[23] R.L. Anderson *et al.*, *Phys. Rev.* **D14**, 679 (1976).
[24] G. Vogel *et al.*, *Phys. Lett.* **B40**, 513 (1972).
[25] D. Drechsel, *Prog. Part. Nucl. Phys.* **34**, 181 (1995).
[26] G. Knöchlein, D. Drechsel, L. Tiator, *Z. Phys.* **A352**, 327 (1995).
[27] R.L. Workman, R.A. Arndt, *Phys. Rev.* **D45**, 1789 (1992).